Eur. Phys. J. B **40**, 439–444 (2004)
DOI: 10.1140/epjb/e2004-00207-9

THE EUROPEAN PHYSICAL JOURNAL B

Weak localization effects in some metallic perovskites

G. Herranz[1,a], F. Sánchez[1], B. Martínez[1], J. Fontcuberta[1], M.V. García-Cuenca[2], C. Ferrater[2], M. Varela[2], and P. Levy[3]

[1] Institut de Ciència de Materials de Barcelona, Campus de la UAB, 08193 Bellaterra, Catalunya, Spain
[2] Departament de Física Aplicada i Òptica, Universitat de Barcelona, Diagonal 647, 08028 Barcelona, Catalunya, Spain
[3] Departamento de Física, CAC, CNEA, Av. Gral Paz 1499 (1650), San Martín, Buenos Aires, Argentina

Received 16 December 2003
Published online 13 July 2004 – © EDP Sciences, Società Italiana di Fisica, Springer-Verlag 2004

Abstract. We report a systematic study of the low-temperature electrical resistivity of epitaxial nanometric $SrRuO_3$ and $LaNiO_3$ thin films. Weak localization effects were taken into account in order to explain the presence of minima in the ρ–T curves. This description can be rationalized by the fact that, at the given growth conditions, the mean free path was comparable to the Fermi wavelength of the carriers, so that effects arising from quantum interference of the electronic wavefunctions were expected. The results reported here are of special interest to understand the relevance of weak localization effects in oxides.

PACS. 72.15.Rn Localization effects (Anderson or weak localization) – 72.80.Ga Transition-metal compounds – 73.50.Bk General theory, scattering mechanisms

1 Introduction

The description of the transport properties in metals is usually based on the Boltzmann theory, according to which the carriers are described from a semiclassical approach. This description is valid in the limit $k_F l \gg 1$, that is, the mean free path l must be far larger than the wavelength $\lambda_F = 2\pi/k_F$ of the carrier wavefunctions in order to describe them as quasi-particles having a definite moment $\vec{k}$ and a position $\vec{r}$. However, when the above condition is violated, new interesting phenomena can arise due to the inherent wavelike nature of the carriers when the mean free path is similar to the wavelength of the carrier wavefunctions. Particularly, one should expect that effects coming from the interference of the quantum wavefunctions should be relevant, leading to what is known in the literature as weak localization effects (WLE) [1–3]. These effects are taken into account by adding a temperature-dependent quantum correction term to the Boltzmann conductivity, that in the case of the weak disorder limit is of order $\sim(k_F l)^{-1}$.

WLE are originated by the constructive interference of the carrier wavefunctions as the carriers are backscattered coherently through the material by a random distribution of scattering centers. There are three relevant lengths to be considered in order to have significant WLE, namely, the Fermi wavelength (λ_F), the mean free path (l) and the inelastic mean free path (l_{in}). The relevance of the last parameter appears due to the fact that the wave coherence has to be kept at long enough distances in order to have a significant interference. During the inelastic collisions, the wave coherence is lost in inelastic collisions due to electron-electron, electron-phonon or electron-magnon interactions. Therefore, in order to have a long enough inelastic mean free path, the temperature must be low enough, that is, WLE are usually observed at low temperature. The occurrence of WLE is signaled by the presence of minima in the resistivity–temperature (ρ–T) curves. On one hand, as the temperature decreases, the wave coherence of the carriers is enhanced, and WLE are reinforced, leading to an enhancement of the resistivity. On the other hand, as the temperature rises, the wave coherence is progressively lost and WLE are weakened, while the normal metallic behaviour is gradually recovered.

WLE are affected by magnetic fields, since their presence modifies the coherence of the carrier wavefunctions, modifying the relevance of the quantum interference effects. The theory predicts typical magnetic field functional dependences for the magnetoresistance coming from WLE [1–3]. Thus, the occurrence of quantum interference effects can be tested by analyzing the field dependence of the magnetoresistance.

In the following, a brief review of previous works on WLE analysis in a variety of materials is given. The reader can consult reference [3] and references therein for further information.

WLE have been proposed to explain the low temperature transport properties of doped semiconductors as Si:P [4] or Ge:Sb [5]. In this case, the carrier density is typically $n < 10^{20}$ cm^{-2}, far below what is commonly found in good metals. Since the carrier wavelength goes as $\lambda_F \alpha n^{-1/3}$, we have $\lambda_F \gg a$, where a is the lattice

[a] e-mail: gherranz@icmab.es

parameter. Since WLE depend on the λ_F/l ratio (see below Eq. (1)), quantum interference effects are enhanced in these materials.

In alloys and composites such as Au-Pd, Cu-CuO, Al-Al_2O_3, $Au_{1-x}Ge_x$, $Nb_{1-x}Si_x$, transport properties were also analyzed taking into account WLE [3]. In these cases, the metallic matrix is a good conductor with a large mean free path, so that $l \gg a$. But the mean free path is shortened by introducing foreign atoms at random positions and introducing structural disorder. By reducing l, the λ_F/l ratio can be increased and WLE are enhanced.

WLE were also analyzed in ultra-thin metallic films (Cu, Mg, Ag, Au, Pt, with thickness $t < 20$ nm). Now, albeit the mean free path is large, WLE are enhanced because of the drastic reduction of one of the dimensions, which strongly enhances quantum interference.

Finally, oxides show a plethora of interesting phenomena, related to the fact that they are strongly correlated electronic systems, including some of the more challenging questions in condensed matter physics, such as non-Fermi-liquid behaviour, high-T_c superconductivity or colossal magnetoresistance. In some oxides the mean free path calculated from the transport properties is such that we have $k_F l \sim 1$, so that the Ioffe-Regel limit is approached. This occurs because high carrier densities approach those of the good metals while the conductivity is noticeably lower. For instance, this situation is given at high temperature in some oxide compounds like $SrRuO_3$ (SRO) [6,7] or $YBa_2Cu_3O_7$ [8], where even though the mean free path approaches the Fermi wavelength, there is no resistivity saturation, as is seen in other non-oxide compounds. For that reason, these oxides are often nicknamed as bad metals.

On the other hand, the condition $k_F l \sim 1$ can also be accomplished at low temperature, and in these cases deviations from the normal Boltzmann theory due to the coherent backscattering of carriers may become significant. We emphasize that even in samples with a high degree of crystalline order, the mean free path can be intrinsically very short. Indeed, indications of WLE have been reported in $La_{2/3}Ca_{1/3}MnO_3$ samples but their presence was not conclusively demonstrated [9]. The high magnetoresistance of manganites and their strong sensitivity to magnetic disorder are a hindrance to a further verification of WLE by performing extended experiments on magnetoresistance. We can partially overcome these shortcomings using $SrRuO_3$ samples, since it is a ferromagnetic perovskite which has a weaker magnetoresistance due to its far weaker sensitivity to magnetic disorder. Indeed, WLE have been suggested in the past to explain the low-temperature electrical transport properties of SRO thin films [10].

For 3D systems, WLE are given by [1–3]

$$\frac{\sigma - \sigma_0}{\sigma_0} \sim \left(\frac{\lambda_F}{l}\right)^{3/2} \left(\frac{k_B T}{\mu}\right)^{1/2} \quad (1)$$

where $\mu \approx E_F$ is the Fermi energy. Generally, quantum corrections to the electrical conductivity include a term due to the self-intersection of the quantum wavefunctions and another that includes the Coulomb electron – electron interactions renormalized by self-interference effects. In the expression equation (1), only the term containing the e^-–e^- interaction quantum correction is considered, since in this work we are dealing with a strongly correlated electronic system. Indeed, usually this term is clearly stronger than the self-interference term, so that the latter can be neglected in the analysis [3]. Definitely, this was corroborated by the analysis performed on the experimental results on our samples, as explained below, and so the self-interference term was dropped from the model.

2 Objectives

We have scrutinized the low-temperature transport properties of $SrRuO_3$ (SRO) thin films by fitting their electrical conductivity to the WLE model described by equation (1). The relative strength of the quantum effects was modulated by modifying the microstructure by changing slightly the growth conditions. In particular, in a series of films, the cooling rate down to room temperature from deposition temperature was changed. In another series, the films were grown on substrates having different miscut angles. In this way, the mean free path could be tuned, so that the λ_F/l ratio was varied. The analysis confirmed that WLE explain the presence of minima in $\rho(T)$ curves at low temperature. The role of disorder on these quantum effects has been also evidenced by creating defects artificially by bombarding with Ar^+ ions. Signatures of field suppressed WLE have been observed in magnetotransport measurements on SRO thin films. It turns out that the coexistence of negative magnetoresistance associated with the ferromagnetic character of SRO may overcome WLE, thus making difficult to discriminate between these two effects. We attempt to overcome these difficulties by extending the WLE analysis to another oxide, $LaNiO_3$ (LNO), which in contrast to SRO doesn't show any magnetic correlation. It is shown that the low-temperature $\rho(T)$ curves can be successfully fitted to the model described by equation (1) both in SRO and in LNO thin films.

3 Low-temperature analysis of the conductivity in $SrRuO_3$ thin films

Films used in this work were grown on $SrTiO_3$ substrates by pulsed laser deposition with a KrF excimer laser ($\lambda = 248$ nm, $\tau = 34$ ns). The oxygen pressure during the deposition was set to 0.1 mbar and the substrate temperature to 750 °C. Experimental details of the growth conditions and the structural characterization can be found elsewhere [11–13]. Since it is relevant for the following discussion, we should mention here the existence of a growth mode transition from an initial 3D-growth to a final 2D-growth in SRO thin films grown on nominally zero-miscut STO(0 0 1) substrates. The initial 3D-growth induces the formation of finger-like structures along well defined directions following the substrate steps. As the thickness

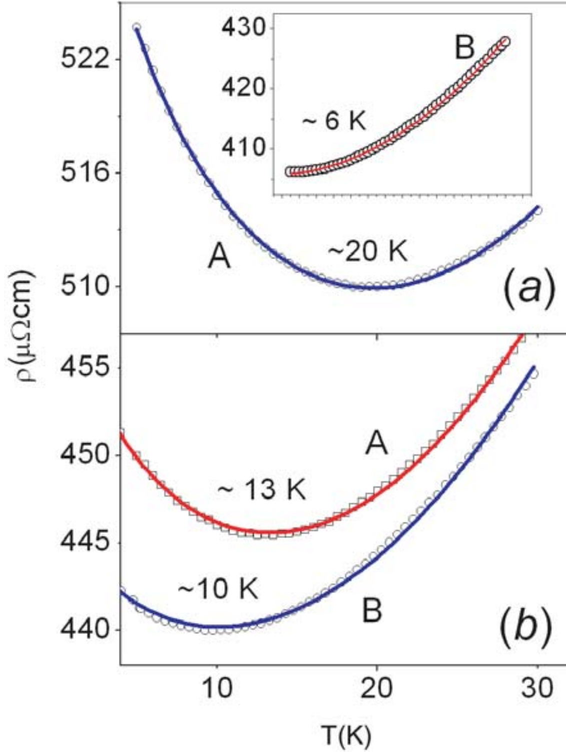

Fig. 1. Plot of the resistivity against the temperature for (a) two samples cooled down to room temperature at different rates (A slow, B fast). In (b), the two samples were grown on two $SrTiO_3$ substrates having different miscut angles (A $\alpha = 0°$, B $\alpha = 2°$). In both figures, fittings to equation (2) are plotted, showing excellent agreement with the experimental data. The temperatures at which the minima appear are written next to the corresponding curves.

increases the finger-like structures eventually coalescence and thereafter the growth proceeds by a 2D step mechanism [13].

As stated above (Eq. (1)), WLE depend on the ratio λ_F/l and, therefore, quantum corrections can be modulated by modifying the mean free path l. With the aim of controlling l, we have modified the microstructure by different methods which will be discussed in the following. We must emphasize that microstructural disorder was varied without altering the chemical composition of SRO.

In one series of films, the microstructure has been controlled by changing the cooling rate from the film deposition temperature down to room temperature [12]. This could be achieved by varying the gas pressure of the growth chamber when the sample was cooled down to room temperature after film deposition. A low-pressure O_2– or Ar– atmosphere implied a slow cooling rate, whereas a high-pressure O_2– or Ar– atmosphere implied a faster cooling rate. As observed in Figure 1a, two films having nearly equal thickness clearly display different residual resistivities depending on the cooling rate, being smaller that corresponding to the film cooled down faster (B, $t = 6$ nm). No significant differences were observed between cooling in O_2 or in Ar, hence the cooling rate is essentially the only relevant parameter. These results can be rationalized by the results reported from the analysis of the temperature dependence of the bulk SRO crystallographic structure by synchrotron X-ray diffraction [14]. This study reveals that a series of polymorphic transitions occur within the temperature range 300 K $\leq T \leq$ 950 K. We suggested [12] that at the regions where the initial elongated structures coalesce the strain relief can stabilize a polymorphic phase which is different from that present in the regions inside the islands. Thus, the amount of disorder could be influenced by the cooling rate after the deposition. Within the context of this paper, it is important to observe that the film having a higher resistivity shows the resistivity minimum at a higher temperature, revealing the significance of disorder in the low-temperature transport properties.

As an alternative method of modifying the film microstructure, we have grown SRO thin films on $SrTiO_3$ substrates having different vicinalities. It is well known that the microstructure of the SRO thin films is strongly influenced by the miscut angle of the substrates [15]. Indeed, in view of the observed growth mode transition from 3D- to 2D-growth, one should expect that the coalescence of the initial islands should occur at a different stage for different substrate miscut angles. In fact, the finger-like structure has the same periodicity as that of the substrate steps and thus, if the width of the substrate steps varies, the coalescence will take place at a different stage [13]. Thus, the density of defects should depend also on the substrate vicinality. In Figure 1b, the resistivity of two films with the same thickness $t = 6$ nm, but grown on substrates with different miscut angle, one on nominally $\alpha = 0°$ (A) and the other with $\alpha = 2°$ (B) is shown. As evidenced by this picture, the film grown on the most vicinal substrate has a lower residual resistivity, implying that in this film the structural disorder is smaller. In close analogy with the results reported above, the film with higher residual resistivity showed the resistivity minimum at a higher temperature.

The properties of the low-temperature transport properties of the previous samples were analyzed on the scope of WLE, by fitting the experimental $\rho(T)$ curves according to the following equation [12]

$$\rho = \frac{1}{\sigma_0 + aT^{1/2}} + bT^2. \quad (2)$$

In addition to the quantum corrected resistivity term, a term in T^2 is included in addition to quantum corrections to account for high temperature scattering contribution. The discussion of the T^2 term is out of the scope of this paper and we will concentrate on the $aT^{1/2}$ term accounting for the quantum corrections.

Fittings of the experimental $\rho(T)$ data according to equation (2) were performed in the 5 K $\leq T \leq$ 30 K temperature range, and are displayed in Figure 1. Note that as the residual resistivity increases, that is, as the microstructural disorder is increased, the physical mechanisms lying behind the occurrence of minima in $\rho(T)$ are enhanced, since they are shifted to higher temperatures.

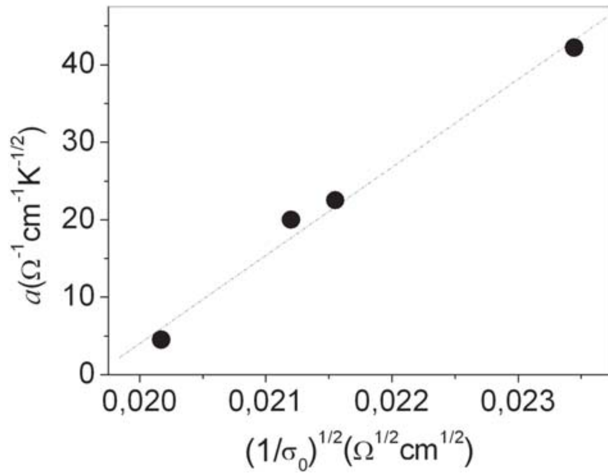

Fig. 2. The coefficient a of the weak localization $T^{1/2}$ term is plotted against $\sigma_0^{-1/2}$, where σ_0 is the residual conductivity.

Thus, it seems that WLE are reinforced when the mean free path is shortened, and this is accomplished by modulating the microstructural disorder.

This observation can be further confirmed by considering the theoretical dependence of the quantum correction term a on the residual conductivity σ_0:

$$a = \lambda_F^4 \left(\frac{ne^2}{h}\right)^{3/2} \frac{(2m^* k_B)^{1/2}}{h} \sigma_0^{-1/2}. \quad (3)$$

From equation (3) it follows that the a values, obtained from the fittings to the experimental data, should display a linear dependence when plotted against $(\sigma_0)^{-1/2}$. As shown in Figure 2, this is the observed behaviour. From the slope of the data displayed in Figure 2, the Fermi wavelength can be estimated (see Eq. (3)), since the other parameters are known (the effective mass of the carriers can be estimated to $m^* \approx 3.7\ m_e$ from Ref. [16]). From this analysis it comes out that $\lambda_F \approx 2$ Å, that is close to the theoretic value $\lambda_F \approx 4.5$ Å, hence giving further support to our analysis.

The quantum correction theories corresponding to weak localization which have been applied here to analyze the conductivity at low temperature are valid provided that they are much smaller than the Boltzmann conductivity, i.e., that $\delta\sigma = aT^{1/2} \ll \sigma_0$. The results of the fittings show that in the studied interval of temperatures ($5\ K < T < 30\ K$), the highest ratio is $\delta\sigma/\sigma_0 \sim 0.1$, so we can reliably use the weak disorder limit for the quantum corrections presented above.

An alternative way to probe further the role of disorder and to probe its relevance on quantum interference effects, is to create defects artificially by irradiating samples with ions. In our case, we started from samples with thickness $t = 20$ nm grown consecutively in identical growth conditions. Resistivity measurements indicated that the virgin films did not have any minimum in ρ(T) for $T > 5$ K. These samples were susbsequently bombarded using a Varian 200 keV implanter (at the laboratory from the Centro Nacional de Energía Atómica

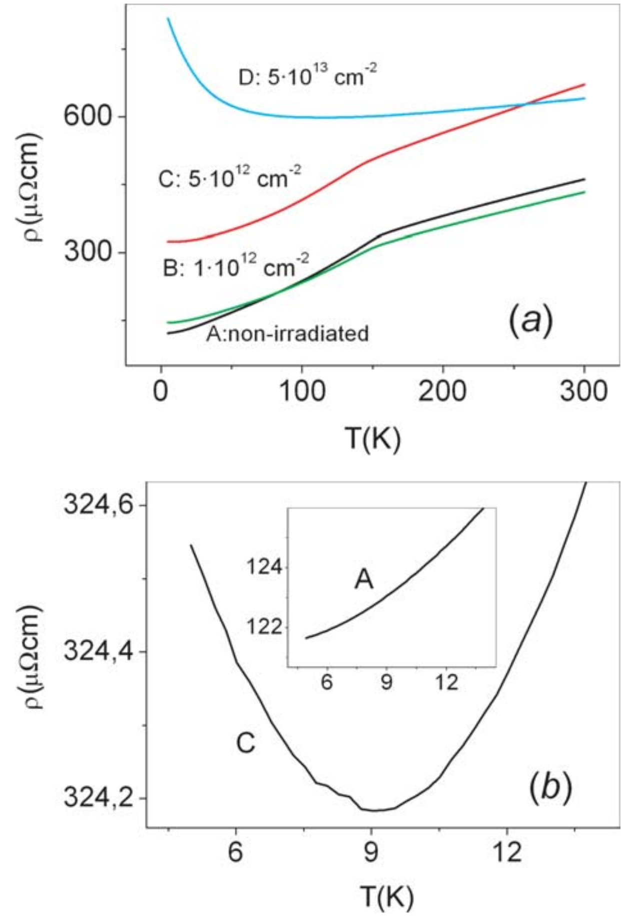

Fig. 3. The $\rho(T)$ curves for SRO samples irradiated at different doses are plotted in (a) The $\rho(T)$ curve labelled as A corresponds to the resistivity of sample C before irradiation. In (b) the low-T region is zoomed for curves A and C (and therefore belongs to the *same* sample).

(CNEA-CAC), Buenos Aires, Argentina) with Ar^+ ions having an energy $E = 100$ keV at different irradiation doses. The effect of the ion irradiation can be seen in Figure 3a, where the ρ(T) curves for different doses are plotted, showing that at some particular doses a minimum appears at $T > 5$ K. Thus, bombarding a SRO sample with a dose of 5×10^{12} Ar^+ ions cm^{-2} promotes the presence of a minimum at $T \sim 10$ K (see Fig. 3b). However, for lower doses (1×10^{12} Ar^+ ions cm^{-2}), although there is an increase of the resistivity, no minimum above 5 K is found and for higher doses the samples became insulating ($\geq 1 \times 10^{13}$ Ar^+ ions cm^{-2}). Therefore, the same trends as observed in the previous set of measurements in SRO thin films are confirmed.

4 Field-dependence of the magnetoresistance in $SrRuO_3$ thin films

To further probe the relevance of quantum corrections to the conductivity in our SRO thin films, measurements under zero and applied magnetic fields were done. As

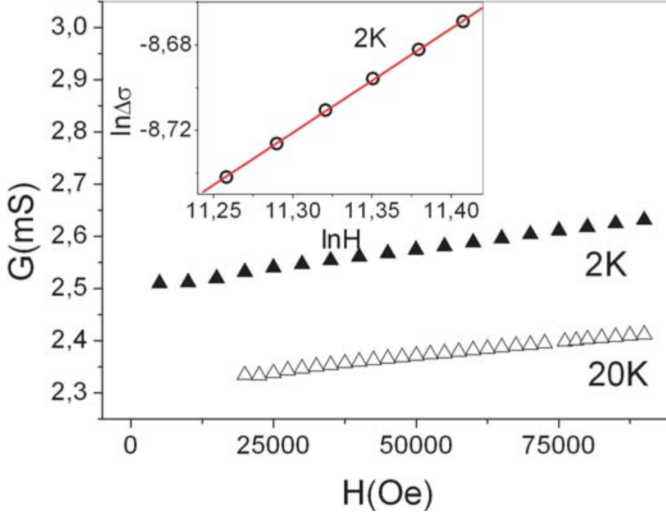

Fig. 4. The magnetic field–dependence of the conductivity measured at $T = 2$ K and at $T = 20$ K are displayed. These measurements correspond to a film with thickness $t = 6$ nm showing a minima in the resistivity at $T_{min} \sim 10$ K. In the inset, the $\ln\Delta\sigma(H,T) = \ln(\sigma(H,T) - \sigma(0,T))$ experimental points corresponding to the measurement at $T = 2$ K were fitted to equation (5) against $\ln H$ in the range 75 kOe $< H <$ 90 kOe.

discussed above, magnetoresistance measurements may confirm the presence of WLE through specific field dependences.

The experiments were carried out by applying a magnetic field perpendicular to the film plane, that is, near the easy magnetic axis [17]. Thus, we minimized other magnetoresistive contributions, such as the anisotropic magnetoresistance (AMR), which is experimentally known to be particularly strong in SRO due to the strong spin-orbit coupling in this compound. We performed an analysis of the field-dependence of the magnetoresistance at fields 5 T $< |H| <$ 9 T, since the field needed to saturate the SRO thin films is above 2 T [18]. Any contribution coming from Hall effect was minimized by changing the polarity of the applied field at each value and suppressing the antisymmetric part of the voltage. The experimental field-dependent magnetoconductance MR(H) data were recorded at different temperatures in the interval 2 K $\leq T \leq$ 35 K. In Figure 4 we can see the MR(H) curves measured at $T = 2$ K and at $T = 20$ K, for a film with thickness $t = 6$ nm, showing a minimum at $T_{min} \sim 10$ K. Thus, the data displayed in Figure 4 corresponds to measurements performed clearly below and above the resistivity minimum, respectively. The expected behaviour for 3D-systems in which WLE are suppressed by an applied magnetic field follows this dependence [3]:

$$\Delta\sigma(H,T) = \sigma(H,T) - \sigma(0,T) = f(x)(eH/h)^{1/2} \quad (4)$$

where $x = hc/(4eHl_{in}^2)$ and l_{in} is the inelastic mean free path, which is temperature-dependent, and $f(x)$ is a smooth function of x (see Ref. [3]). For $x \ll 1$, the function $f(x)$ tends to a constant. It can be easily estimated that for $H \sim 100$ kOe the previous condition is satisfied provided that $l_{in} \gg 10$ nm. We can rewrite equation (4) into

$$\ln\Delta\sigma(H,T) = \ln(f(x)) + (1/2)\ln(e/h) + (1/2)ln(H). \quad (5)$$

The $\ln\Delta\sigma$ of the curve corresponding to the measurement at $T = 2$ K was fitted to equation (5) against $\ln H$ in the range 75 kOe $< H <$ 90 kOe, and the resulting fitting is displayed in the inset to Figure 4. The slope obtained from the $\ln\sigma - \ln H$ linear fit is $m = 0.489$ in contrast to the value $m = 0.5$ expected from equation (5). Thus, it would seem that in the interval of fields analyzed, the function $f(x)$ remains essentially constant and the main contribution comes from the $\ln H$ term. Hence, one could easily attribute the $MR(H)$ dependence to the suppression of the wave coherence by the applied magnetic field.

However, these considerations must be taken with caution. SRO is a ferromagnetic compound and, thus, it has a large internal magnetic field and, therefore, it should be expected that high fields are needed in order to actually modify the coherence of the wavefunctions. With these precautions in mind, we remark in Figure 4 that the $MR(H)$ curves measured at $T = 2$ K $< T_{min}$ and at $T = 20$ K $> T_{min}$ are both negative and increase with field at similar rates. That means that the phenomena that lead to such magnetocoductance are very similar above and below the temperature T_{min} at which the minimum appears. Thus, these experiments do not allow to discriminate between the contributions to the magnetoresistance coming from the suppression of WLE and from other sources. Probably, in order to determine the contribution of WLE to the magnetoresistance, the application of substantially higher magnetic fields than the used here are required.

5 Low-temperature analysis of the conductivity in $LaNiO_3$ thin films

At this point, $LaNiO_3$ (LNO) appears as a good candidate to check all these effects, since it is a metallic oxide with no magnetic correlations. Indeed, in the past WLE have been put forward to explain the transport properties at low temperature of LNO bulk polycrystalline samples [19,20]. In these works, the analysis of the low-temperature dependence of the electrical conductivity, magnetic field–dependence of magnetoresistance measurements and tunneling experiments supported the assumption of the presence of WLE in this oxide. However, it must be noted that the samples under that study were polycrystalline in nature, and that a significant contribution coming from grain boundaries could be present. In our case, we performed transport measurements on high-quality epitaxial LNO thin films and, thus, such contribution could be avoided.

LNO thin films on $LaAlO_3$ (0 0 1) substrates have been prepared by pulsed laser deposition. Details of the growth conditions and structural characterization can be found elsewhere [21]. Under certain growth conditions,

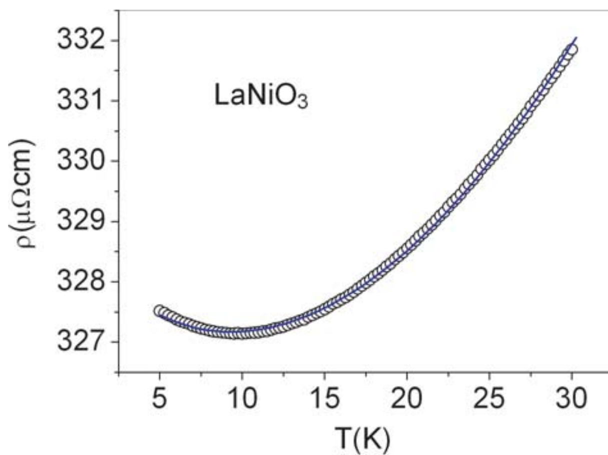

Fig. 5. Plot of $\rho(T)$ of a $LaNiO_3$ thin film with thickness $t \approx 240$ nm showing a minimum at ∼10 K. The figure also shows the fitting to equation (2).

minima in the $\rho(T)$ curves appeared, and they were analyzed following the same procedure as in SRO thin films. The solid line through the experimental points in Figure 5 shows the result of a fitting of $\rho(T)$ at low temperature (5 K $\leq T \leq$ 30 K) using equation (2) for a LNO film with thickness $t \approx 240$ nm, grown at $T = 600$ °C and in a pressure of 0.1 mbar. The fitting is excellent, and it seems to indicate the occurrence of WLE in our LNO samples. Extensive details of the fitting procedure and the significance of the extracted parameters from the fittings will be reported separately. Here we would like just to emphasize that LNO thin films appear as optimal candidates to carry on more measurements to probe the relevance of quantum corrections to the conductivity.

6 Conclusions and perspectives

We have focused on the low-temperature transport properties of $SrRuO_3$ and $LaNiO_3$ thin film oxides. We suggest that the presence of minima in the ρ(T) curves can be explained by quantum corrections to the conductivity coming from weak localization effects. The results reported here will help to understand the relevance of these quantum corrections in strongly correlated metallic systems such as the present oxides.

At the same time, we have emphasized the role of disorder in the relevance of WLE, which modulates the relative strength of quantum corrections through the tuning of the mean free path. The essential contribution to the WLE comes from Coulomb electron – electron interactions renormalized by self-interference effects. Thus, in addition, we evidenced the influence of disorder on the electron – electron interactions.

More experiments are in perspective. Studies of the magnetic-field dependences of the magnetoresistance should be relevant to probe further the scope of WLE in our thin films. In this view, LNO thin films are optimal, since they do not show magnetic correlations and, thus, the contributions of magnetoresistive effects other than WLE can be avoided.

We acknowledge financial support from the MCyT (Spain) project MAT2002-04551-C03 and MAT2003-4161. We acknowledge also the CNEA's (Centro Nacional de Energía Atómica, Buenos Aires, Argentina) Ion Implantation Laboratory Staff.

References

1. P.A. Lee, T.V. Ramakrishnan, Rev. Mod. Phys. **57**, 287 (1985)
2. B.L. Altshuler, A.G. Aronov, in *Electron-electron interaction in disordered conductors*, edited by A.L. Efros, M. Pollak (North-Holland, Amsterdam, 1985)
3. A. Abrikosov, *Fundamentals of the theory of metals* (North-Holland, Amsterdam, 1988)
4. T.F. Rosenbaum, K. Andres, G.A. Thomas, P.A. Lee, Phys. Rev. Lett. **46**, 568 (1981)
5. G.A. Thomas, A. Kawabata, Y. Ootuka, S. Katsumoto, S. Kobayashi, W. Sasaki, Phys. Rev. B **26**, 2113 (1982)
6. P.B. Allen, H. Berger, O. Chauvet, L. Forro, T. Jarlborg, A. Junod, B. Revaz, G. Santi Phys. Rev. B **53**, 4393 (1996)
7. L. Klein, J.S. Dodge, C.H. Ahn, G.J. Snyder, T.H. Geballe, M.R. Beasley, A. Kapitulnik, Phys. Rev. Lett. **77**, 2774 (1996)
8. V.J. Emery, S.A. Kivelson, Phys. Rev. Lett. **74**, 3253 (1995)
9. M. Auslender, A.E. Kar′kin, E. Rozenberg, G. Gorodetsky, J. Appl. Phys. **89**, 6639 (2001)
10. M.A. López de la Torre, Z. Sefrioui, D. Arias, M. Varela, J. E. Villegas, C. Ballesteros, C. León, J. Santamaría, Phys. Rev. B **63**, 052403 (2001)
11. G. Herranz, B. Martínez, J. Fontcuberta, F. Sánchez, M.V. García-Cuenca, C. Ferrater, M. Varela, Appl. Phys. Lett. **82**, 85 (2003)
12. G. Herranz, B. Martínez, J. Fontcuberta, F. Sánchez, C. Ferrater, M.V. García-Cuenca, M. Varela, Phys. Rev. B **67**, 174423 (2003)
13. F. Sánchez, M.V. García-Cuenca, C. Ferrater, M. Varela, G. Herranz, B. Martínez, J. Fontcuberta, Appl. Phys. Lett. **83**, 902 (2003)
14. B.J. Kennedy, B.A. Hunter, J.R. Hester, Phys. Rev. B **65**, 224103 (2002)
15. J.C. Jiang, W. Tian, X.Q. Pan, Q. Gan, C.B. Eom, Appl. Phys. Lett. **72**, 2963 (1998)
16. P.B. Allen, H. Berger, O. Chauvet, L. Forro, T. Jarlborg, A. Junod, B. Revaz, G. Santi, Phys. Rev. B **53**, 4393 (1996)
17. L. Klein, J.S. Dodge, C.H. Ahn, J.W. Reiner, L. Mieville, T.H. Geballe, M.R. Beasley, A. Kapitulnik, J. Phys.: Condens. Matter **8**, 10111 (1996)
18. K.S. Takahashi, A. Sawa, Y. Ishii, H. Akoh, M. Kawasaki, Y. Tokura, Phys. Rev. B **67**, 094413 (2003)
19. N. Gayathri, A.K. Raychaudhuriy, X.Q. Xu, J.L. Peng, R.L. Greene, J. Phys.: Condens. Matter **10**, 1323 (1998)
20. K.P. Rajeev, A.K. Raychaudhuri, Phys. Rev. B **46**, 1309 (1992)
21. F. Sánchez, C. Ferrater, C. Guerrero, M.V. García-Cuenca, M. Varela, App. Phys. A **71**, 59 (2000)